Evidence for Strain Glass in the Ferroelastic-Martensitic System $Ti_{50-x}Ni_{50+x}$

Shampa Sarkar,[1] Xiaobing Ren,[1,*] and Kazuhiro Otsuka[1]

[1]*Materials Physics Group, National Institute for Materials Science, 1-2-1 Sengen, Tsukuba 305-0047, Japan*

(Received 23 May 2005; published 8 November 2005)

We report here "strain glass," a new glassy phenomenon in ferroelastic-martensitic system of Ni-rich intermetallic $Ti_{50-x}Ni_{50+x}$ ($x > 1$), where local strain is frozen in disordered configuration below a critical temperature T_g. The ac elastic modulus shows a minimum at T_g, which exhibits logarithmic frequency dependence following Vogel-Fulcher relationship, and the corresponding internal friction shows a frequency-dependent peak located at a lower temperature. *In situ* high-resolution transmission electron microscopy observations reveal uncorrelated nanoclusters of martensiticlike phase, randomly frozen in the otherwise untransformed parentlike matrix. Being parallel to spin glass and relaxor, strain glass may shed new light on the fundamental physics of glass and lead to the discovery of novel properties.

DOI: 10.1103/PhysRevLett.95.205702 PACS numbers: 64.70.Pf, 61.43.Fs, 62.20.Dc, 64.70.Kb

"Glass" [1] is a generic term for a frozen state of an essentially disordered system with local order only. It characterizes a wide range of complex systems from physics to biology. In general, a system tends to transform into a glassy state rather than into a long-range ordered configuration when there exist random defects and frustrations. The most common glassy systems, viz., the spin glass [2,3] (in magnetic system) and the ferroelectric relaxor [4] (in electric-dipolar system) have been discovered and studied for many decades. However, the existence of glassy phenomenon in another physically parallel system, viz., ferroelastic [5,6] or martensite (where lattice strain is the order parameter), has remained unclear.

Earlier simulations by Kartha *et al.* [7,8] suggested that the crosshatched tweed patterns [9,10] appearing prior to martensitic transformation in Fe-Pd or Ni-Al can be considered as a strain glass phase. However, this view faces difficulty to explain a large body of well-known experimental observations that over the entire temperature regime of the tweed there exists no dip/peak in elastic-modulus/loss-tangent, nor frequency dispersion of these properties [11]. These mechanical-susceptibility anomalies are necessary experimental evidences to prove a "strain" glass, just like similar anomalies in magnetic susceptibility proving the existence of a "spin" glass. On the other hand, certain mixed cyanides (e.g., KCN-KBr, etc.) have been reported to exhibit a dip in elastic constant c_{44} and frequency dispersion in dielectric susceptibility [Ref. [12] and references therein]. These systems have been identified as "orientational glass," as the glass state is characterized by a freezing of different orientations of the ellipsoidal CN^- molecular ions. Although the glassy behavior of these cyanides seems to satisfy some of the necessary conditions for strain glass, their nature has remained controversial [12] due to the complications by the inevitable coupling of strain with electric dipoles/quadruples of CN^- molecular ions [13], as evidenced by the simultaneous anomalies in both elastic and dielectric susceptibility [12]. In this Letter, we report direct evidences for the existence of a glassy martensite or "strain glass," in a metallic system of Ni-rich, off-stoichiometric intermetallic Ti-Ni. The newly discovered glass may enrich the physics of glasses and may lead to metallic materials with novel properties.

A martensitic transformation [5,6,14] is a self-organization phenomenon in solid, where the atoms move diffusionlessly below a transition temperature (M_s); this causes spontaneous distortion to an otherwise undistorted high-symmetry lattice and results in a low-symmetry phase, called martensite. Thus, martensitic transformation can be viewed as a long-range ordering of elastic strain below M_s, with strain being the order parameter [14] [the long-range strain order is the origin of the important "shape memory effect" [11]]. This is analogous to the ordering of magnetic moments in a ferromagnet [2] or electric dipoles in a ferroelectric [4], below their corresponding Curie temperature T_c. Being symmetry lowering and first order in nature, the martensitic transition proceeds with nucleation and growth of different martensite-variants (or domains) of the same structure and energy, but of different orientations [15]. The strain variants self-organize spontaneously in the martensite state to minimize transformation strain energy [5,14].

For near-equi-atomic Ti-Ni shape memory alloy, there exist two competing routes [11] for martensitic transformation from the high-symmetry parent $B2$ lattice (ordered body-centered cubic): (i) $B2 \rightarrow B19'$ (monoclinic), which is a strongly first-order martensitic transformation with maximum lattice deformation $\sim 10\%$, or (ii) $B2 \rightarrow R$ (trigonal), a weakly first-order transformation with only $\sim 1\%$ lattice deformation. The preferential occurrence of $B2 \rightarrow R$ over $B2 \rightarrow B19'$ transformation can be achieved by creating hindrance to the formation of $B19'$ martensite. The R phase may (or may not) transform further to $B19'$ martensite, depending sensitively on the strength of such hindrance.

Figure 1 depicts the temperature-composition (T-c) phase diagram for as-quenched $Ti_{50-x}Ni_{50+x}$ alloys, which were solution treated at 1273 K for 1 h and then quenched rapidly in water (WQ). The phase diagram shows that the martensitic transformation for near-stoichiometric compo-

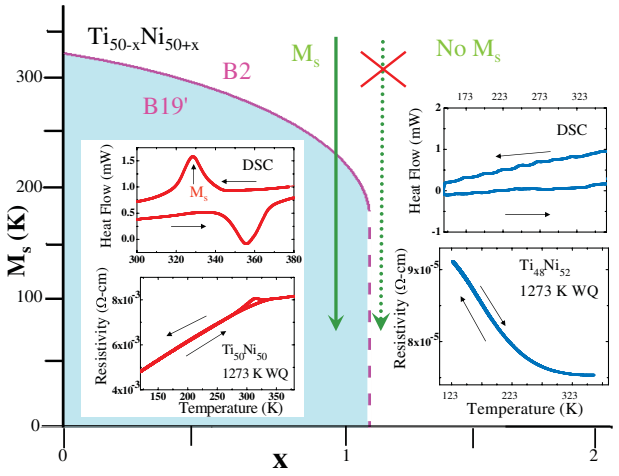

FIG. 1 (color). Temperature-composition (T-c) phase diagram for as-quenched $Ti_{50-x}Ni_{50+x}$, bisected into regions of appearance (blue region) and disappearance of $B2 \rightarrow B19'$ martensitic transformation; the border composition is slightly above $Ti_{49}Ni_{51}$. The $B2 \rightarrow B19'$ transformation, appearing as an enthalpy peak in differential scanning calorimetry (DSC) measurement and resistivity $\rho(T)$ drop in ρ vs T measurement for $Ti_{50}Ni_{50}$, vanishes abruptly for $x > 1$. The $\rho(T)$ curve for $Ti_{48}Ni_{52}$ exhibits negative temperature dependence $d\rho/dT < 0$, being similar to the case of R-phase formation, but there is no signature for a long-range $B2 \rightarrow R$ transformation. Here WQ stands for "water quenched."

sitions ($x \leq 1$) commences via the $B2 \rightarrow B19'$ route. However, for Ni-rich, off-stoichiometric compositions with $x > 1$, a twofold mystery arises: (i) the robust $B2 \rightarrow B19'$ martensitic transformation is suppressed bewilderingly and (ii) a signature of R-martensite-like phase (rather than $B19'$-like phase) appears in the electrical resistivity curve $\rho(T)$, as $\rho(T)$ increases continuously with decreasing temperature (which characterizes R formation). But no trace of long-range R phase has been found in this temperature regime [16]. Here we show that Ni-rich off-stoichiometric $Ti_{50-x}Ni_{50+x}$ (for $x > 1$) actually transforms into a "strain glass" (glassy-R martensite) phase, which can be achieved from the inherent site randomness provided by point defects (excess Ni atoms occupying randomly Ti sites), and competition and conflicts amongst various competing, localized strain variants with similar ground state energies. The combination of such randomness and equally accessible, competing strain variants produces frustration, where the system transforms (freezes) into a configuration of uncorrelated nanoclusters of martensitic R-like phase, distributed randomly in parent $B2$ matrix.

As dynamics plays a crucial role in the freezing process of a glassy transition, the most common experimental technique is the measurement of the frequency dependence of a relevant dynamical variable in a temperature window spanning glass transition. For magnetic systems [i.e., spin glass [2]], such an experimental tool is the measurement of the frequency dependence of the ac magnetic susceptibility; for electric-dipolar systems [ferroelectric relaxor or dipole glass [4]], it is the frequency dependence of the ac electric permittivity measurement. The corresponding measurement for martensitic (or strain) system, as pointed out earlier, is the mechanical-susceptibility measurement, or the dynamical mechanical analysis, which measures the ac elastic compliance (normally its inverse quantity, ac elastic/storage modulus) and the loss (called internal friction) at different frequencies.

The frequency ω dependence of the ac storage modulus $S(\omega)$ and the internal friction $Q^{-1}(\omega)$ measurements were performed on a dynamic mechanical analyzer (Q800 from TA Instruments) in infrasonic frequency range (0.1 Hz to 10 Hz). Polycrystalline Ti-Ni samples (60 mm $\times$ 10 mm $\times$ 0.8 mm in size) were measured in a dual cantilever mode by applying a small ac bending stress, which generated a maximum sample displacement of $\sim$20 μm.

Very interestingly, the temperature dependence of the ac storage modulus $S(\omega, T)$ for the "nontransforming" $Ti_{48.5}Ni_{51.5}$ shows a dip, where the associated internal friction $Q^{-1}(\omega, T)$ exhibits maximum slope, followed by a peak at lower temperature [see Figs. 2(a) and 2(b)]. The existence of a dip in the ac storage modulus clearly suggests a phase transition; however, the transitional dip in $Ti_{48.5}Ni_{51.5}$ has important differences from that of a long-range strain-ordered martensitic transformation, as seen in Figs. 2(c) and 2(d). First, the dip height of $S(\omega, T)$ is significantly lower than that of a normal, long-range-ordered (martensitic) transforming composition ($Ti_{50-x}Ni_{50+x}$ for $x \leq 1$), and decreases pronouncedly with increasing defect concentration x (i.e., excess Ni atoms) [see Fig. 2(d)]. Second and most remarkably, the dip temperature T_g for $Ti_{48.5}Ni_{51.5}$ exhibits logarithmic frequency dependence; i.e., the dip broadens, decreases in magnitude, and shifts to higher temperature logarithmically with increasing frequency [Figs. 2(a) and 2(b)]. This important feature, being characteristic of a glass transition, is absent for a long-range-correlated martensitic transformation for $Ti_{50-x}Ni_{50+x}$ with $x \leq 1$ [see Fig. 2(c), which is $Ti_{49}Ni_{51}$ and shows normal martensitic transformation], which does not exhibit frequency dependence of the dip temperature for such low frequency range. Exactly similar behaviors as seen in Fig. 2(a) have been observed previously for the real part of ac susceptibility for spin glasses and ferroelectric relaxor in the similar low/audio frequency range [2,4].

The frequency shift ($\Delta\omega$) of $T_g(\omega)$ in such frequency range is quantified by the parameter $\Delta T_g/[T_g(\Delta \log\omega)]$, which has a value of $\sim$0.02 for Ni-rich Ti-Ni specimen. This value for $Ti_{50-x}Ni_{50+x}$ ($x > 1$) is very similar to the values obtained for spin glasses [2]. We have further fitted the non-Arrhenius ω dependence of $T_g(\omega)$ [see inset of Fig. 2(a)] using empirical Vogel-Fulcher law [2], $\omega = \omega_0 \exp[-E_a/k_B(T_g - T_0)]$. The best fit gives E_a (activation barrier) to be $\sim$150 K, $\omega_0 \sim 10^5$ s^{-1}, and $T_g/T_0 \sim 1.1$ for $Ti_{48.5}Ni_{51.5}$, where T_0 is called "ideal-glass" temperature.

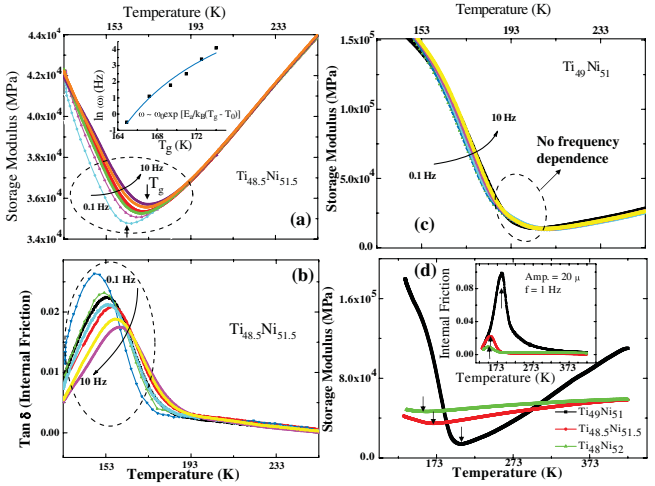

FIG. 2 (color). (a) and (b) show temperature dependence of ac storage modulus $S(\omega, T)$ and internal friction $Q^{-1}(\omega, T)$ for the "nontransforming" $Ti_{48.5}Ni_{51.5}$, respectively, at various frequencies (0.1 Hz–10 Hz). Although the DSC and $\rho(T)$ measurements suggest the "absence" of martensitic transformation for such specimen, $S(\omega, T)$ produces a dip at T_g [as shown in (a)], which has logarithmic frequency dependence and the corresponding $Q^{-1}(\omega, T)$ exhibits a maximum at lower temperature [as seen in (b)]. By contrast, the storage modulus $S(\omega, T)$ for transforming ($B2 \rightarrow B19'$) specimen ($Ti_{49}Ni_{51}$, quenched from 1123 K) shows no frequency dependence of the dip temperature (c). The dip height of $S(\omega, T)$ decreases by an order of magnitude with increasing Ni content just by 1% (i.e., samples with more chemical disorder), exhibiting influence of disorder towards suppressing the long-range strain ordering (martensitic transformation) (d). Inset of (a) shows the "non-Arrhenius" T_g vs $\ln(\omega)$ curve for $Ti_{48.5}Ni_{51.5}$, fitted well by the Vogel-Fulcher equation, a signature of most glass transitions. All the samples were water quenched (WQ) from high temperature to ensure a homogenous solid solution.

We note here that the above features in the mechanical susceptibility cannot be explained by any known alternative effects, e.g., long-range strain-ordering transition [like ferroelastic-martensitic transition or certain incommensurate-commensurate transition [17]] or domain wall dynamic effect, because the former effect cannot explain the observed large frequency dispersion in mechanical susceptibility and the latter effect cannot explain the existence of a modulus minimum.

To microscopically characterize the features of this new transition, *in situ* high-resolution transmission electron microscopy (HREM) observations were performed on a series of $Ti_{50-x}Ni_{50+x}$ specimens for $0 \leq x \leq 2$, by varying the temperature from 298 K to 95 K. The $Ti_{50}Ni_{50}$ (and up to $x = 1$) specimen shows well-developed $B19'$ domain morphologies (see Fig. 4) below their corresponding $B2 \rightarrow B19'$ transformation temperatures, indicating a long-range strain ordering, as observed previously [5,11]. However, for $Ti_{50-x}Ni_{50+x}$ ($x > 1$), the diffraction pattern at 298 K [Fig. 3(a)] shows some additional, very faint, diffuse superlattice reflections, appearing at incommensurate positions near $(0 \quad 1/3 \quad 1/3)_{B2}$ (usually called 1/3 spots) along with the $B2$ parent reflections. As the superlattice spots at exact 1/3 commensurate position indicate the formation of long-range strain-ordered R phase [5,18], the diffuse and faint incommensurate spots reflect the tendency to form a R-like martensitic phase.

The comparative study of these superlattice spots at a fixed temperature also exhibits an interesting characteristic trend: they are sharper with higher intensity and appear closer to 1/3 commensurate position for specimen with lower Ni-content, i.e., lower defect concentration. With the temperature lowering, the 1/3-like diffuse spots became sharper and shift towards commensurate 1/3 position [Fig. 3(a)]; however, never reach exact commensurate 1/3 value and are "frozen" in that incommensurate position at a temperature consistent with T_g, where the corresponding ac storage modulus $S(\omega, T)$ produces the dip. The most interesting observations come from the corresponding temperature dependence of the high-resolution dark-field images [Fig. 3(b)], which reveal many uncorrelated, tiny nanodomains of size 1–5 nm, distributed randomly in the $B2$-like matrix at room temperature. The nanodomains grow in size (up to 20–25 nm) with decreasing temperature; however, get frozen in those configurations below T_g and do not grow any further, thereby preventing the formation of a cooperative martensitic phase with long-range strain order.

These uncorrelated nanoclusters can be considered as a "frustrated" configuration, but the origin of the frustration needs to be clarified. One likely source of the frustration is

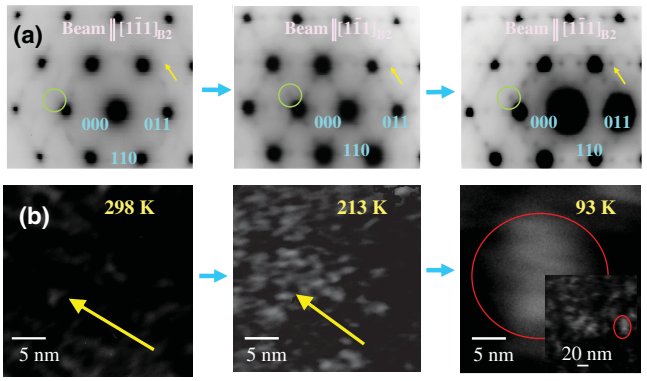

FIG. 3 (color). Electron diffraction pattern of $[1\bar{1}1]_{B2}$ zone axis for $Ti_{48}Ni_{52}$ is shown as a function of temperature in (a). The diffuse superlattice reflections at incommensurate 1/3 position (marked by yellow arrow), which is almost invisible at room temperature, become sharper and of higher intensity with lowering temperature; however, do not change below 158 K (T_g for $Ti_{48}Ni_{52}$) and fail to reach commensurate 1/3 value (which is characteristic of a long-range ordered R phase). The corresponding HREM dark-field images (b), obtained by using the reflections marked by green circle in (a), reveal random distribution of tiny nanodomains of R-like phase in $B2$-like matrix. The nanodomains grow to some extent in size but are finally frozen in that configuration.

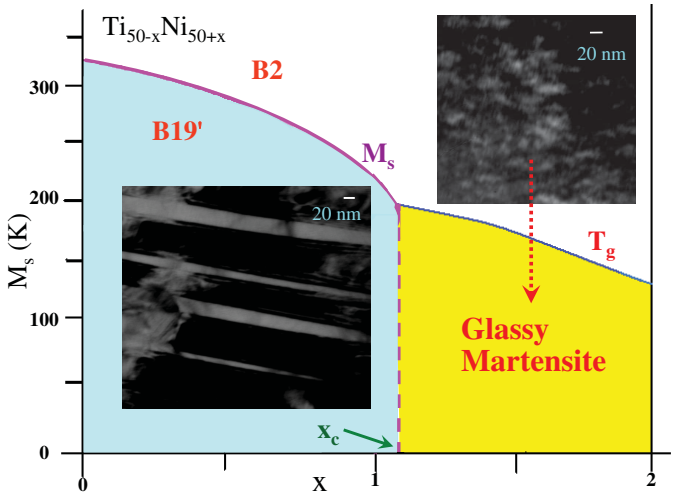

FIG. 4 (color). Modified temperature-composition (T-c) phase diagram for as-quenched Ni-rich $Ni_{50-x}Ni_{50+x}$, where the "glassy-martensite" phase is mapped in the yellow region, separated by a dashed line from the long-range correlated $B19'$ martensitic phase (blue region). Two TEM images, one with large domains of $B19'$ phase (for specimen undergoing long-range strain-ordered $B2 \rightarrow B19'$ transformation) and one with tiny nanodomains (for "glassy-martensite" specimen), have been shown on a comparative ground. x_c is the threshold concentration of excess Ni, above which the as-quenched $Ti_{50-x}Ni_{50+x}$ transforms into the glassy phase.

the conflicts amongst eight energetically equivalent strain variants [of $B2(Pm3m) \rightarrow R(P3)$ transformation] at random point defect sites (excess Ni at Ti sites). We mention here that the mechanism of glass formation in ferroelastic systems has been recently described theoretically by Toledano *et al.* [19]. They described very similarly the frustrated multidomain state for paraelastic $\rightarrow$ ferroelastic transition, which can explain the amorphization process under pressure in several systems like Cs_2HgBr_4, α quartz, ice, etc. Hence, due to the random point defects and multiple possibilities to form strain variants, self-organization and collective growth of the strain variants to form a long-range strain ordering can be suppressed. Below certain temperature T_g, these frustrated nanodomains may be frozen into a "glassy state," which has no long-range correlation. We term this glassy phase as "strain glass" and this is the first experimental evidence for a glassy phase in metallic martensite.

The modified T-c phase diagram for $Ti_{50-x}Ni_{50+x}$ based on our new findings is sketched in Fig. 4. M_s represents the onset temperature of long-range $B2 \rightarrow B19'$ martensitic transformation, which decreases sharply with increasing x for $0 > x \geq 1$. Above a threshold Ni excess value x_c ($x_c \sim 1$), the strain glass regime appears, which has a glassy R phase, rather than a glassy-$B19'$ phase, as indicated by diffraction evidence (i.e., 1/3-like reflections in Fig. 3). The details about the preferential occurrence of glassy R over glassy $B19'$ will be described elsewhere [20].

In conclusion, we report here the discovery of a glass with a surprisingly new origin: a frozen local strain order in a class of metallic systems that have martensitic or ferroelastic instability, which normally undergo long-range strain ordering [5,6,11,14,15] at transformation temperature. However, this new glassy martensite (strain glass) fails to reach the long-range strain order and freezes in a state, in which short-range strain order persists. The origin of the strain glass can be attributed to site randomness caused by excess Ni atoms and certain frustration, but the exact nature of the frustration needs further investigation. The new discovery may open a new research field and may lead to metallic materials with novel properties, like spin glass [2] or ferroelectric relaxor [4] did.

This work was supported by Sakigake-21 of Japan Science and Technology Agency and Kakenhi of JSPS. S. S. acknowledges JSPS for Grant No. P03507. We thank G. L. Fan, Y. Wang, and F. X. Yin for technical support in DMA measurement.

*Corresponding author.
Email address: Ren.Xiaobing@nims.go.jp

[1] C. A. Angell, Science **267**, 1924 (1995).
[2] J. A. Mydosh, *Spin Glasses* (Taylor & Francis, London, 1993).
[3] J. Snyder, J. S. Slusky, R. J. Cava, and J. R. Schiffer, Nature (London) **413**, 48 (2001).
[4] B. E. Vugmeister and M. D. Glinchuk, Rev. Mod. Phys. **62**, 993 (1990).
[5] *Shape Memory Materials*, edited by K. Otsuka and C. M. Wayman (Cambridge University Press, Cambridge, England, 1998).
[6] K. Otsuka and T. Kakeshita, MRS Bull. **27**, 91 (2002).
[7] S. Kartha, T. Castan, J. A. Krumhansl, and J. P. Sethna, Phys. Rev. Lett. **67**, 3630 (1991).
[8] S. Kartha, J. A. Krumhansl, J. A. Sethna, and L. K. Wickham, Phys. Rev. B **52**, 803 (1995).
[9] F. Pérez-Reche, B. Tadic, L. Manosa, A. Planes, and E. Vives, Phys. Rev. Lett. **93**, 195701 (2004).
[10] A. Saxena, T. Castan, A. Planes, M. Porta, Y. Kishi, T. A. Lograsso, D. Viehland, M. Wuttig, and M. De Graef, Phys. Rev. Lett. **92**, 197203 (2004).
[11] K. Otsuka and X. Ren, Prog. Mater. Sci. **50**, 511 (2005).
[12] U. T. Hochli, K. Knorr, and A. Loidl, Adv. Phys. **39**, 405 (1990).
[13] K. H. Michel, Phys. Rev. Lett. **57**, 2188 (1986).
[14] A. G. Khachaturyan, *Theory of Structural Transformation in Solids* (Wiley, New York, 1983).
[15] G. R. Barsch, B. Horovitz, and J. A. Krumhansl, Phys. Rev. Lett. **59**, 1251 (1987).
[16] T. Kakeshita *et al.*, Jpn. J. Appl. Phys. **37**, 2535 (1998).
[17] A. V. Kityk, V. P. Soprunyuk, A. Fuith, W. Schranz, and H. Warhanek, Phys. Rev. B **53**, 6337 (1996).
[18] D. Shindo, Y. Murakami, and T. Ohba, MRS Bull. **27**, 121 (2002).
[19] P. Toledano and D. Machon, Phys. Rev. B **71**, 024210 (2005).
[20] S. Sarkar, X. Ren, and K. Otsuka (to be published).